

·土木工程·

DOI:10.12454/j.jsuese.202301011



本刊网刊

“L”形槽不出筋叠合板承载性能足尺试验研究

刘威^{1,2}, 郭小农¹, 文艺³, 王兵², 周森², 徐军³, 戴靠山^{3*}

(1. 同济大学土木工程学院, 上海 200092; 2. 上海宝冶集团有限公司, 上海 200941; 3. 四川大学土木工程系, 四川 成都 610065)

摘要:针对传统叠合板外伸钢筋严重影响施工质量和效率的问题,提出“L”形不出筋叠合板端部设计新方法,该方法采用预设“L”形槽孔来放置板边、板间的连接钢筋,避免了板端出筋,具有制作、储运、施工方便等优势,可大幅提高施工效率。为探究该“L”形槽端部设计方法对板梁连接处的整体性以及叠合板承载性能的影响,本研究采用堆载的方式对 6 个带端梁的足尺楼板试件进行了静载试验,其中,3 个“L”形槽不出筋叠合板、2 个传统叠合板以及 1 个同尺寸现浇整板。采用应变采集仪、高精度位移计和裂缝观测仪获得了试件关键部位的试验数据,如端部“L”形钢筋、传统叠合板端部伸出钢筋的应变,叠合板跨中挠度,跨中裂缝宽度、间距等并进行了分析。结果表明:“L”形槽配合“L”形筋的结构设计可起到与传统纵向钢筋一致的连接效果,其“L”形钢筋弯折与“L”形槽相互作用限制了板端部钢筋的滑移,虽然“L”形钢筋长度较短,较传统伸出钢筋与后浇混凝土黏结强度也略低,其仍然能有效传递荷载;新型端部构造对板的跨中承载力影响微小,“L”形槽不出筋叠合板与传统叠合板的力学性能总体相近,满足正常使用极限状态和承载能力极限状态性能要求。通过试验初步验证了“L”形槽不出筋叠合板构造设计的可行性。

关键词:不出筋叠合板;足尺试验;“L”形槽;力学性能;板梁连接

中图分类号: TU375.2; TU317.2

文献标志码: A

文章编号: 2096-3246(2025)06-0213-09

装配式建筑是一种基于预制构件和模块化设计原理的建筑方式,相较于传统现浇式建筑具有快速施工和能耗降低等优点,在现代建筑领域中受到越来越多的关注^[1-4]。作为装配式建筑结构的主要构件,叠合板因其具有高可靠性、快速施工能力和质量可控等优点,成为当前最常用的混凝土楼板类型。

叠合板是由预制板和后浇层叠合而成的装配整体式楼板,通常由一层预制混凝土底板和一层后浇钢筋混凝土组成^[5-7]。在实际工程中,楼板通常由多块叠合板拼接而成并连接到边梁,楼板作为直接承受楼面荷载的构件,其拼缝和板梁连接处的性能最为关键^[8-10]。为了保证拼缝和板梁连接界面的整体性,传统叠合板的预制底板在制作时需要预留外伸钢筋,在后浇施工时将其同板梁连接在一起。但外伸钢筋不仅不利于构件的搬运、堆叠和运输,在此过程中钢筋的弯曲、折断、锈蚀等问题也对现场施工、构件质量和结构强度造成困扰。

近年来,针对外伸钢筋问题,国内外学者提出了多种解决方案,多采用分离式拼缝(密拼拼缝)作为解决途径。《装配式混凝土连接节点构造》(15G310—1)^[11]给出了分离式拼缝(图集称密拼拼缝)的连接构造方法。吴方伯等^[12]提出一种新型拼缝构造措施,发现拼缝处设置的抗裂钢筋能有效抑制拼缝的开展,并提高其极限承载力;任彧等^[13]为研究密拼拼缝对板支反力传递路径的影响,对均布荷载作用下密拼拼缝叠合板受力机理进行了研究,发现密拼拼缝叠合板的整体破坏形式仍趋于双向板受荷下的破坏形式;余泳涛等^[14]对单缝密拼钢筋混凝土叠合板受弯性能进行了试验研究,提出了双向叠合板密拼拼缝的设计建议和构造要求;何庆锋等^[15]提出一种增强型密拼拼缝构造,并对其受力性能进行试验研究,结果表明其承载能力接近于现浇板,并能保证拼缝处力的有效传递。密拼拼缝虽然能解决叠合板间连接可靠性问题,但仍未能从根本上解决施工便利性问题,其更高标准的施工工艺还会在一定程度上增加施工难度。

收稿日期:2023-12-10 修回日期:2024-06-27 网络出版日期:2024-08-23

基金项目:四川省重点研发项目(2023YFS0427)

作者简介:刘威(1984—),男,博士生,高级工程师。研究方向:装配式建筑和低碳技术。E-mail:2280092@tongji.edu.cn

*通信作者:戴靠山,教授,E-mail:kdai@scu.edu.cn

不出筋叠合板是近年来提出的一种解决外伸钢筋问题的新方案,因其灵活的构造形式而受到广泛关注^[16-19]。章雪峰等^[20]提出一种四边不出筋密拼连接叠合板,并对其进行试验研究,验证了该新型构造能满足正常使用和承载能力极限状态要求。肖宇等^[21]提出了阶梯拼缝和弧型螺栓拼缝两种新型构造,并对其进行了静力加载试验,结果表明,两种新型拼缝可以防止拼缝处的裂缝沿叠合面横向发展而过早破坏,抗弯刚度和承载力随钢筋屈服强度的增大及后浇层厚度的增大而增大,并提出了两种新型拼缝配筋设计方法。江海华等^[22]提出一种板端不出筋平板叠合板,对其进行力学性能试验和数值模拟,论证了板端不出筋的可行性,并提出相关工程设计建议。

上述研究表明,不出筋叠合板能够实现与传统出筋叠合板等同的承载能力,但目前研究大多集中于板间拼缝连接,对结构整体性能同样有着显著影响的板梁连接处则缺乏足够关注。为此,本文提出了一种构造相对简单、施工更加便捷的“L”形槽不出筋叠合板端部设计新方法,并对其板梁连接处的整体性及其连接方式对楼板力学性能的影响进行足尺试验研究,开展了5个两端带端部梁的叠合板以及1个相同尺寸现浇整板足尺试件的堆载试验。

1 试件概况

1.1 试件参数

试验共设计制作了6个足尺试件,其中,新型“L”形槽不出筋叠合板S1(以下简称新型板)3个,传统叠合板S2(以下简称传统板)2个,现浇板SIS 1个,试件差别主要为板端部的连接构造方式,具体参数如表1所示。构造方式1为新型板采用的“L”形筋端部构造,方式2为传统板和现浇板采用的传统出筋构造方式,两种构造方式如图1所示。每个新型板一端布置6个“L”形槽,共计12个,槽短边长为200 mm,长边长为230 mm,槽深为20 mm,宽为30 mm,槽间距为300 mm;在槽内放置1根 $\Phi 10$ 的“L”形钢筋,6个“L”形槽内的钢筋截面总面积约为 4.71 cm^2 ,与原板底部9根间距为200 mm纵向受力 $\Phi 8$ 钢筋截面总面积 4.52 cm^2 基本相当,浇筑混凝土后与边梁连接成整体,“L”形筋与板底部纵筋竖向位置关系见图1(d)。各试件尺寸均为3 500 mm(长) \times 1 800 mm(宽) \times 130 mm(厚);与板两端相连接的边梁截面为2 200 mm(长) \times 300 mm(宽) \times 600 mm(高)。采用C30混凝土,实测其立方体抗压强度 $f_{\text{cu,k}}=37.4 \text{ MPa}$,弹性模量 $E_c=3.2 \times 10^4 \text{ MPa}$;采用HRB400E级钢筋,其常温实测结果见表2。

表1 试件设计参数

试件编号	端部构造	现浇板厚/mm	预制板厚/mm
S1-1	方式1	70	60
S1-2	方式1	70	60
S1-3	方式1	70	60
S2-1	方式2	70	60
S2-1	方式2	70	60
SIS	方式2	130	0

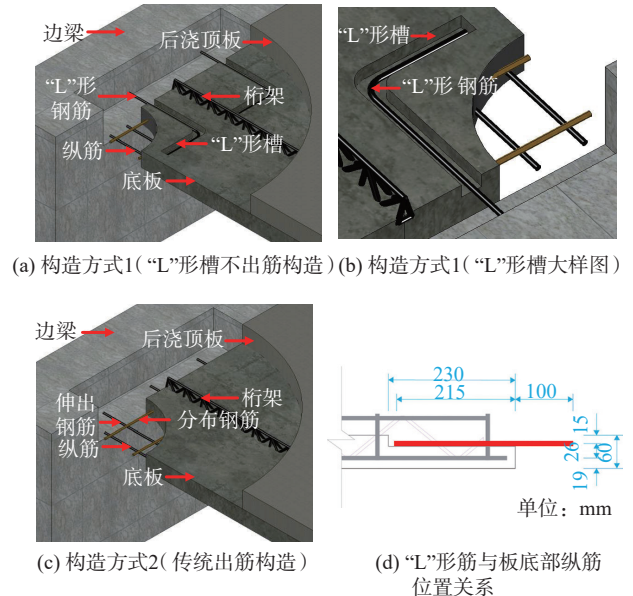


图1 端部构造方式

Fig. 1 End construction approach

表2 钢筋力学性能

钢筋种类	f_y/MPa	f_t/MPa	δ
$\Phi 8$	460	600	13.5
$\Phi 10$	415	620	15.0
$\Phi 12$	415	585	16.5
$\Phi 16$	440	605	16.5

注: f_y 为钢筋屈服强度, f_t 为钢筋抗拉强度, δ 为钢筋最大力总伸长率。

1.2 加载方案

加载方案参照《混凝土结构试验方法标准》(GB/T 50152—2012)^[23]。因现场试验条件限制,采用堆载加载方式,每个配重块重900 kg,楼板单层可以堆放9个配重块,采用中心对称的加载顺序如图2所示,每次加2个配重块,加满18块之后每次加1块,堆满1层后按此顺序继续堆载第2层,每个配重块的吊装时间间隔为5 min。堆载现场如图3所示。

试件承载能力极限状态判别标志:1)受拉主筋拉断;2)受压区混凝土压碎或混凝土应变达到0.003 3;

3) 跨中挠度达到计算跨度的 1/50;4) 最大裂缝宽度达到 1.5 mm。本次试验所有试件均在受拉区最大裂缝宽度达到 1.5 mm 时判定为达到承载能力极限状态, 停止加载。

7	8	4
1	3	2
5	9	6

图 2 配重块加载顺序

Fig. 2 Sequence of loading counterweight blocks



图 3 堆载现场

Fig. 3 On site loading

1.3 量测内容

试验的量测内容: 1) 配重块的加载数量; 2) 板中和梁上部的竖向位移、梁下部水平位移; 3) 受力钢筋应变; 4) 板跨中和梁板交界面的裂缝宽度。在叠合板上、下皮钢筋粘贴应变片; 在板端、跨中和边梁外侧及顶部布置位移计, 观察试件受力变形以及边梁与板端固结的边界条件; 同时在试验时使用裂缝宽度观测仪观测各加载工况下板端和跨中的裂缝宽度。各板位移测点布置相同, 如图 4 所示。“L”形不出筋叠合板应变片布置如图 5(a) 所示, 传统叠合板和现浇板应变片布置如图 5(b) 所示。

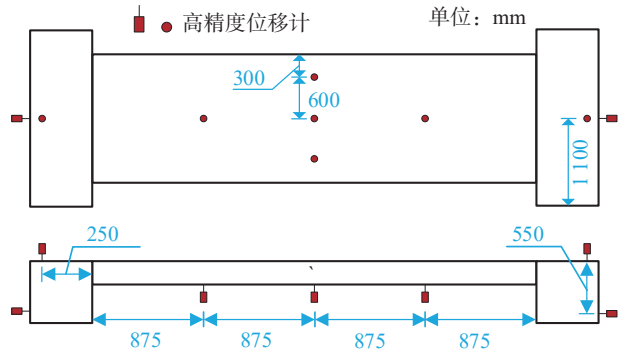
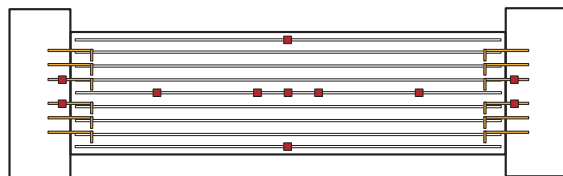
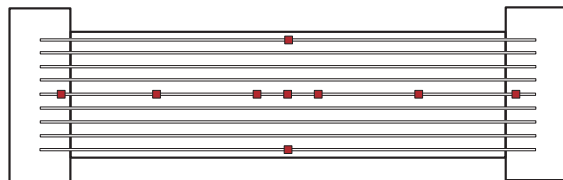


图 4 位移计测点布置

Fig. 4 Layout of displacement gauges



(a) “L”形不出筋叠合板应变片布置



(b) 传统叠合板和现浇板应变片布置

图 5 应变片布置

Fig. 5 Layout of strain gauges

2 试验现象及结果分析

2.1 裂缝

试验中, 将试件跨中裂缝的条数、间距和宽度, 端部裂缝的宽度作为观察指标。对比新型板、传统板和现浇板的裂缝发展情况, 分析这些指标随加载量级的变化规律。

各试件裂缝发展形态如图 6 所示。由图 6(a)、(b) 可看出, 裂缝发展过程相似, 板端部和跨中弯矩最大处首先开裂, 而后随着荷载增加, 跨中裂缝数量和裂缝宽度不断增加, 裂缝间距变小, 裂缝沿横向开展, 呈现出典型的受弯破坏特征。各试件达到承载能力极限状态稳定后, 试件 S1-1、S1-2、S1-3、S2-1、S2-2 和 SIS 的裂缝条数分别为 12、13、15、13、15 和 20 条, 可以看出新型板跨中裂缝条数和传统板相似; 平均裂缝间距为 10.24、11.73、10.91、8.43、10.12 和 7.04 cm。综上所述, 新型板的裂缝条数和裂缝间距均与传统板相似, 而现浇板的裂缝条数明显多于叠合板, 且间距更小。试验结果表明, 新型板跨中的抗弯承载力和变形能力均与传统板接近, 明显高于现浇板。与传统板相比, 新型端部构造并未削弱板跨中的承载性能。

由图 6(c) 可看出, 端部开裂之后裂缝数量始终为 1 条, 位于板梁交界处, 其宽度随荷载增加而增大。主要原因在于板截面高度 130 mm, 远小于梁截面高度 600 mm, 梁截面刚度较大, 故裂缝仅在梁板交界的板截面处, 即刚度突变处出现, 梁上不会再有新的裂缝开展。

事实上, 在竖向荷载作用下, 梁底部有向外侧滑移的趋势, 滑移后会释放部分端部弯矩, 为限制梁底向外侧滑移, 尽可能模拟端部固定铰支座的约束条件, 试验时在梁底部和中部都设置了锚定钢筋, 边梁向外滑移

位移和转角如表 3 所示。由表 3 可知,滑移普遍处于较低水平,其转角计算可采用以下简化公式:

$$\theta = \frac{x}{h} \times \frac{180^\circ}{\pi} \quad (1)$$

式中, θ 为梁的转角, x 为梁底滑移, h 为梁高。其中, 试件 S1-2 最大滑移 5.9 mm 时所引起的端部转动角度约为 0.615°, 由于梁底可以转动, 虽然角度很小, 也可认为端部为铰接约束, 其加载时弯矩分布如图 7 所示。

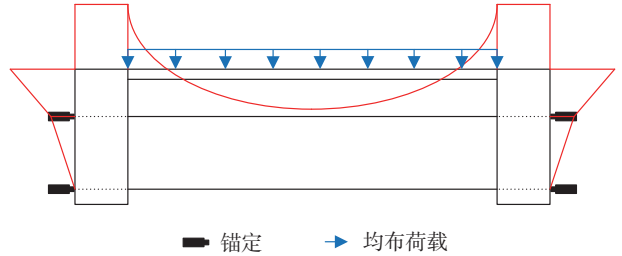


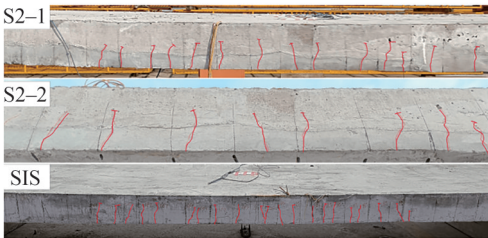
图 7 试件加载时弯矩分布

Fig. 7 Bending moment distribution of the specimen during static loading

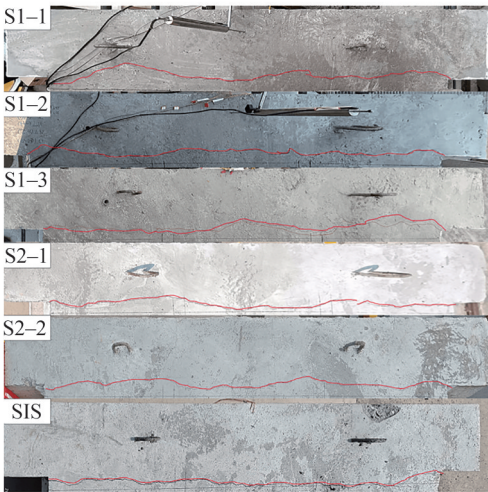
试验中, 新型板在加载到 21.5 kN/m² 时, 板端先开裂, 裂缝垂直于叠合板长度方向; 类似地, 传统叠合板和现浇整板分别在加载 23.8 和 22.4 kN/m² 时板端开裂, 之后随着荷载的增加裂缝数量和宽度不断增加。新型板初裂荷载较小, 说明“L”形端部构造一定程度上降低了试件端部的抗裂性。各试件端部在开裂后到承载能力极限状态时的裂缝宽度随荷载变化关系如图 8 所示, 新型板和传统板的端部裂缝宽度随荷载非线性增加, 且曲线表现相似, 开裂后曲线斜率较小, 裂缝宽度随荷载增加缓慢, 再加载到 28.6 kN/m² 后曲线斜率突然增大, 此时现浇板端部裂缝宽度发展也明显加快, 达到承载能力极限状态限值。加载过程中裂缝总体发展情况如下。



(a) 新型板跨中裂缝发展形态



(b) 传统板和现浇板跨中裂缝发展形态



(c) 板端裂缝发展形态

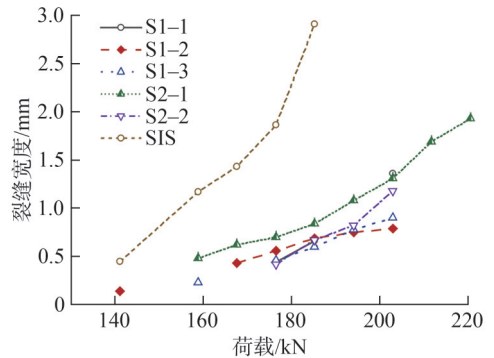
图 6 各试件裂缝发展形态

Fig. 6 Crack development morphology of each specimens

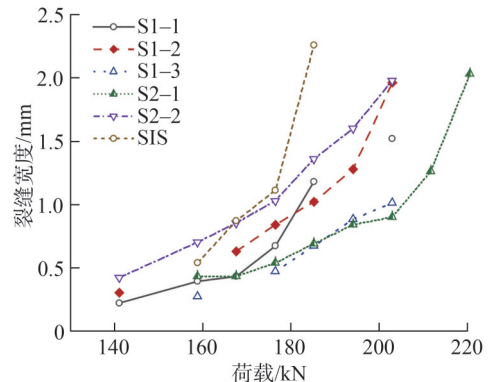
表 3 边梁滑移和转角

Tab. 3 Slip and rotation of the edge beams

试件编号	左端滑移/ mm	左端转角 θ_L /(°)	右端滑移/ mm	右端转角 θ_R /(°)
S1-1	3.9	0.406	3.8	0.396
S1-2	5.9	0.615	0.2	0.021
S1-3	3.4	0.354	0.5	0.052
S2-1	0.9	0.094	0.5	0.052
S2-2	3.1	0.323	2.3	0.240
SIS	0	0	4.3	0.448



(a) 试件左端裂缝宽度随荷载变化情况



(b) 试件右端裂缝宽度随荷载变化情况

图 8 各试件的荷载-裂缝宽度关系曲线

Fig. 8 Load-crack width relationship curves for each specimen

1) 裂缝发展规律:第1种为除现浇板外的5个试件,它们在开裂前期,裂缝数量增加,裂缝宽度随荷载增加较为缓慢,后期裂缝数量发展完全,裂缝间距相似,裂缝宽度发展速度显著加快,直至达到裂缝宽度限值;第2种为现浇板开裂后裂缝便迅速发展至试件破坏。分析原因:开裂后钢筋作为主要受力构件,现浇板因缺少桁架钢筋,板刚度较叠合板小,故裂缝发展迅速,桁架钢筋可以有效增加板抗弯刚度^[24]。

2) 端部裂缝宽度:图8中,在承受 27.9 kN/m^2 的均布荷载时,新型板左端部平均裂缝宽度 0.487 mm ,传统板 0.56 mm ,现浇板 1.86 mm ;新型板右端部平均裂缝宽度 0.66 mm ,传统板 0.78 mm ,现浇板 1.11 mm ;类似地,在每一个裂缝宽度采样点,端部裂缝宽度都表现出新型板与传统板类似且明显优于现浇板的规律,这体现在二者裂缝宽度数据的相似性和曲线斜率变化的一致性上,说明“L”形槽的端部设计在板梁连接处整体性方面与传统叠合板出筋连接效果基本相当。

2.2 挠度

各试件的荷载-挠度曲线变化关系如图9所示,取板跨中挠度作为挠度代表值。从图9可以看到,曲线有两个主要阶段:第1阶段为挠度随荷载线性增加,此时端部和跨中混凝土尚未开裂,试件整体处于弹性阶段;第2阶段为挠度非线性增加,通常在试件出现初始裂缝后,挠度开始迅速增加。

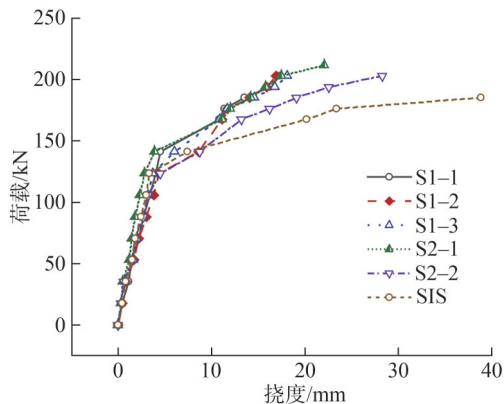


图9 各试件的荷载-挠度关系曲线

Fig. 9 Load-deflection relationship curves for each specimen

从图9还可看出:第1阶段,各类板几乎没有差异;第2阶段,新型板S1-1、S1-2、S1-3跨中最大竖向位移分别为 17.3 、 18.1 、 18.1 mm ,平均值为 17.83 mm ;传统板S2-1、S2-2跨中最大竖向位移分别为 22.1 、 28.3 mm ,平均值为 25.2 mm ;现浇板SIS跨中竖向最大位移为 39.1 mm 。当承受相同荷载为 20.7 kN 时,新型板S1跨中竖向位移平均值为 17.83 mm ,传统板S2为 22.9 mm ,现浇板SIS取极限荷载为 18.9 kN 时竖向

位移为 39.1 mm ,事实上,新型板和传统板在板的结构设计上是相同的,差别只在端部构造,其端部受力变形性能相近,故其跨中挠度发展也相近,新型板的挠度增长速度略小于传统板,并且在达到承载能力极限状态时的挠度也小于传统板,现浇板的刚度最小。综合挠度和裂缝分析来看,与现浇板和传统叠合板相比,端部构造采用“L”形钢筋并不会明显影响叠合板跨中的抗弯刚度。

2.3 应变

各叠合板底板端部与边梁连接处关键钢筋荷载-应变关系如图10所示。图10中,图例20、21为左端钢筋应变片,图例30、31为右端钢筋应变片。

试件底板端部钢筋荷载-应变曲线主要分为两个阶段:第1阶段为受压阶段,在受拉部分混凝土开裂前,根据平截面假定,构件端部受弯截面中性轴以上受拉,以下受压;第2阶段为受拉阶段,受拉部分混凝土开裂后,截面受压区高度减小,使预制底板端部钢筋也开始受拉。

由图10可以看到,各类板端部钢筋应变在试件端部混凝土开裂前均小于0(受压),但绝对值很小,几乎没有随荷载的增加而发生明显变化,混凝土开裂后钢筋应变由负变正并迅速增大,进入屈服阶段。

由此可见,与传统钢筋类似,“L”形钢筋在正常使用阶段,特别是混凝土开裂前,承受压应力很小,对构件端部抗弯承载力贡献也很小。原因在于:端部受负弯矩,在截面中性轴以下为受压部分,压应力主要由受压区混凝土承担,故在上部混凝土开裂前,钢筋受压且应变较小。混凝土开裂后,一方面,混凝土失去抗拉承载力,拉力除了由顶部钢筋承担外,随着受压区高度降低,端部“L”形钢筋也开始承受拉力;另一方面,“L”形钢筋的头部也就是所设计的“L”形弯折限制了钢筋与混凝土的相对滑移,保证钢筋不会被拔出使得叠合板试件结构性失效,这表现在加载后期,如图10(g)所示,新型板的“L”形钢筋和传统板的胡子筋均出现屈服,充分发挥钢筋的承载力,“L”形槽的设计弥补了“L”形钢筋长度较短可能造成的黏结强度低的缺陷。

由图10(g)可以看出,在试件达到承载能力极限状态之前,各试件的端部钢筋均出现屈服,两类构造方式的力学性能表现相似,即“L”形钢筋在进入受拉阶段后仍能有效承载。

各试件板上皮关键钢筋荷载-应变关系曲线如图11所示。由图11可以看到,除现浇板SIS外,各试件上皮钢筋应变随荷载增加幅度较小。新型板上皮关键钢筋与传统板有相似的荷载-应变曲线,现浇板的上皮钢筋应变偏大,导致其现浇板端部裂缝宽度

偏大。主要原因为现浇板缺乏架立钢筋,整体刚度比叠合板小,相同荷载下板变形(主要体现在竖向挠

度)更大,故现浇板上皮钢筋应变明显大于叠合板同位置处钢筋的应变。

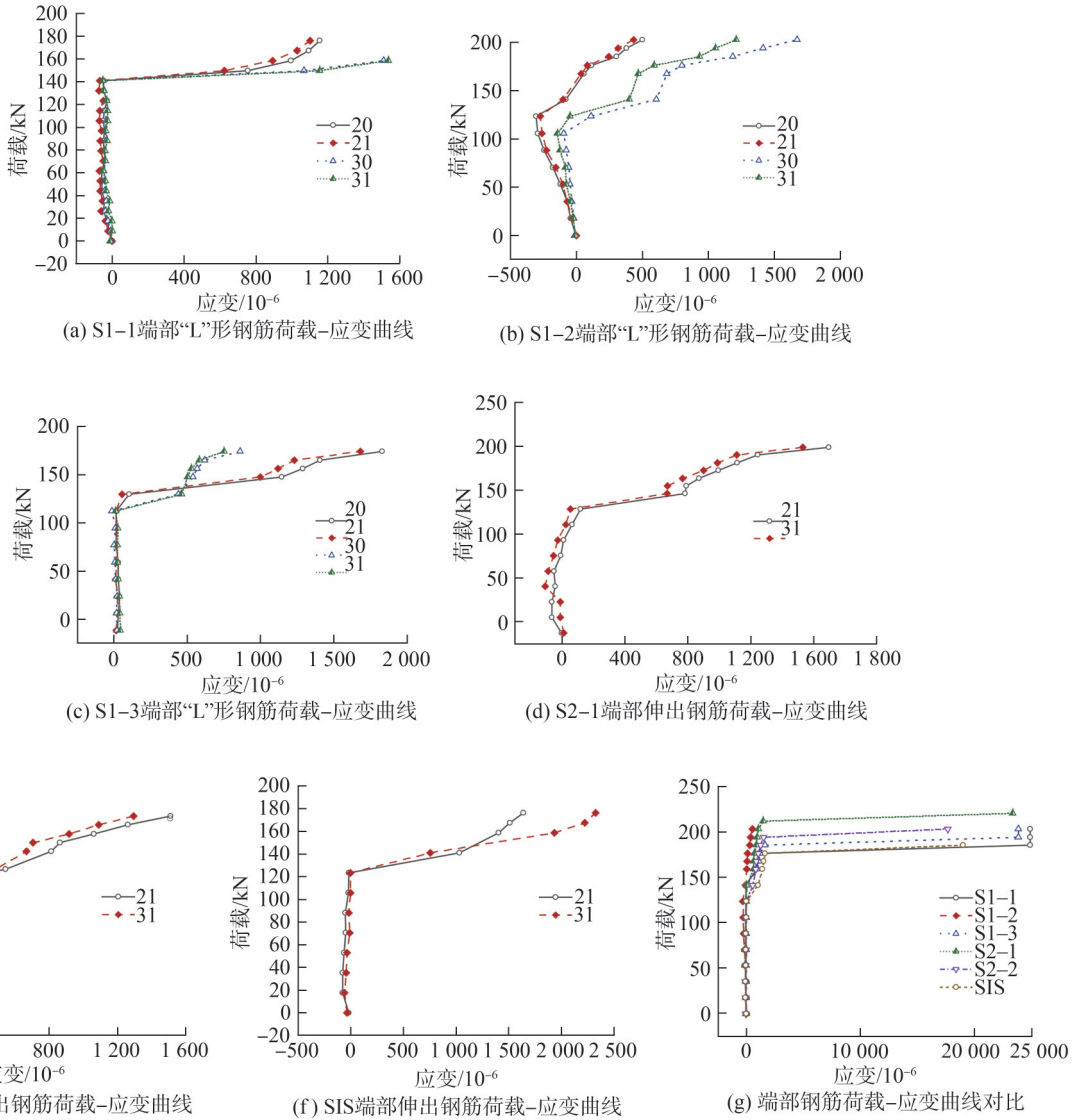


图10 各试件的荷载-应变关系曲线

Fig. 10 Load-strain relationship curves for each specimen

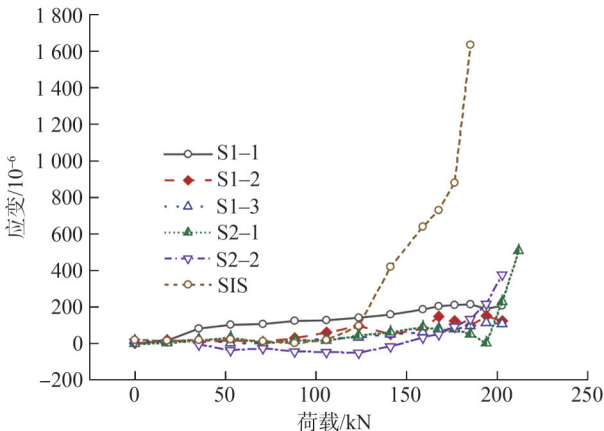


图11 各试件板上皮关键钢筋荷载-应变关系曲线

Fig. 11 Load-strain relationship curves of the key steel bars at the slab top for each specimen

2.4 特征荷载值对比

各试件的开裂荷载和极限荷载实测值如表4所示。由表4可知,新型板开裂荷载较传统板降低约9.5%,极限荷载则基本相同,说明在后浇顶板配筋相同的情况下,底板端部“L”形钢筋的构造设计会在一定程度上降低混凝土的抗裂性,但仍是一般住宅楼板的设计荷载 $2.5\sim 5.0\text{ kN/m}^2$ 的4~8倍,满足正常使用要求。事实上,本文试验以端部裂缝宽度达到1.5 mm作为试件达到承载能力极限状态的标志,传统板和新型板的极限荷载基本相同,表明开裂后裂缝宽度受底板端部钢筋构造形式影响较小;现浇板因刚度较小,端部裂缝发展较快,故极限荷载小于新型板和传统板。

表4 各试件的开裂荷载和极限荷载实测值

Tab.4 Measured values of cracking load and ultimate load for each specimen

试件编号	开裂荷载/(kN·m ⁻²)	极限荷载/(kN·m ⁻²)
S1-1	22.4	32.2
S1-2	19.6	32.2
S1-3	22.4	32.2
S2-1	25.2	33.6
S2-2	22.4	30.8
SIS	22.4	27.9

3 结论

对“L”形槽不出筋叠合板、传统出筋叠合板和现浇板进行了静力堆载试验,得到如下结论:

1)采用“L”形槽后,在加载过程中,新型板与传统板的端部裂缝宽度及分布都非常相似,且明显优于现浇板,说明“L”形端部设计方法能提供足够的板梁连接可靠性。

2)“L”形钢筋的结构设计可以有效承受端部混凝土开裂后传递到其上的拉力,“L”形弯折限制了钢筋与混凝土的相对滑移,确保板端部与主梁的可靠连接,弥补了“L”形钢筋长度较短造成与后浇混凝土黏结强度低的缺陷,保证了结构的安全性。

3)采用“L”形槽后,新型板的承载能力没有明显降低,等同或者基本等同传统出筋叠合板,满足正常使用极限状态和承载能力极限状态要求,初步验证了“L”形槽不出筋叠合板端部设计的可行性。

参考文献:

[1] Huang Xinyi, Shu Zhan, Li Zheng. Research development of prefabricated modular buildings and modular connections[J]. Progress in Steel Building Structures, 2022, 24(2): 40–49. [黄馨仪, 舒展, 李征. 装配式模块化建筑与模块节点研究进展[J]. 建筑钢结构进展, 2022, 24(2): 40–49.]

[2] Ferdous W, Bai Yu, Ngo T D, et al. New advancements, challenges and opportunities of multi-storey modular buildings—A state-of-the-art review[J]. Engineering Structures, 2019, 183: 883–893.

[3] Xiao Xuwen, Cao Zhiwei, Liu Xing, et al. Status, problems and countermeasures of prefabricated buildings in China [J]. Building Structure, 2019, 49(19): 1–4. [肖绪文, 曹志伟, 刘星等. 我国建筑装配化发展的现状、问题与对策[J]. 建筑结构, 2019, 49(19): 1–4.]

[4] Wu Gang, Feng Decheng. Research progress on fundamental performance of precast concrete frame beam-to-column connections[J]. Journal of Building Structures, 2018, 39(2): 1–16. [吴刚, 冯德成. 装配式混凝土框架节点基本性能研

究进展[J]. 建筑结构学报, 2018, 39(2): 1–16.]

[5] Wu Liwei, Chen Haibin, Liu Yibin. Experimental study on static performance of precast concrete composite hollow floors[J]. Journal of Building Structures, 2018, 39(Supp2): 36–42. [武立伟, 陈海彬, 刘亦斌. 混凝土预制叠合空心楼板静力性能试验研究[J]. 建筑结构学报, 2018, 39(增刊2): 36–42.]

[6] 刘洋, 李志武, 杨思忠, 等. 装配式建筑叠合楼板研究进展[J]. 混凝土与水泥制品, 2019(1): 61–68.

[7] 刘轶, 童根树, 李文斌, 等. 钢筋桁架叠合板性能试验和 design 方法研究[J]. 混凝土与水泥制品, 2006(2): 57–60.

[8] Xu Tianshuang, Xu Youlin. An experimental study on transmission properties of joints between superposed slabs[J]. Building Science, 2003(6): 11–14. [徐天爽, 徐有邻. 双向叠合板拼缝传力性能的试验研究[J]. 建筑科学, 2003(6): 11–14.]

[9] Yan Feng, Gao Jie, Tian Chunyu, et al. Experimental study on full-scale superimposed concrete slab with joints[J]. Building Structure, 2016, 46(10): 56–60. [颜锋, 高杰, 田春雨, 等. 带接缝的混凝土叠合板足尺试验研究[J]. 建筑结构, 2016, 46(10): 56–60.]

[10] 周旺华. 现代混凝土叠合结构[M]. 北京: 中国建筑工业出版社, 1998.

[11] 中国建筑标准设计研究院. 装配式混凝土结构连接节点构造: 15G310—1[S]. 北京: 中国计划出版社, 2015.

[12] Wu Fangbo, Liu Biao, Li Jun, et al. Experimental study and finite element analysis of structural measures for joints between new type of superposed slabs[J]. Industrial Construction, 2015, 45(2): 50–56. [吴方伯, 刘彪, 李钧, 等. 新型叠合板拼缝构造措施的试验研究及有限元分析[J]. 工业建筑, 2015, 45(2): 50–56.]

[13] Ren Yu, Yang Yuxing, Xu Peitao, et al. Mechanical mechanism and finite element analysis of laminated slab with split-joint under uniform load[J]. Building Structure, 2023, 53(17): 119–126. [任彧, 杨昱幸, 徐沛韬, 等. 均布荷载作用下密拼缝叠合板受力机理及有限元分析[J]. 建筑结构, 2023, 53(17): 119–126.]

[14] Yu Yongtao, Zhao Yong, Gao Zhiqiang. Experimental research on flexural behavior of reinforced concrete composite slab connected without gap[J]. Journal of Building Structures, 2019, 40(4): 29–37. [余泳涛, 赵勇, 高志强. 单缝密拼钢筋混凝土叠合板受弯性能试验研究[J]. 建筑结构学报, 2019, 40(4): 29–37.]

[15] He Qingfeng, Hu Chengqun, Yang Kaihua, et al. Experimental study on joint structure and mechanical performance of densely assembled composite slabs[J]. Journal of Hunan University(Natural Sciences), 2022, 49(3): 111–122. [何庆锋, 胡程群, 杨凯华, 等. 密拼叠合板拼缝构造及受力性

- 能试验研究[J]. 湖南大学学报(自然科学版),2022,49(3): 111–122.]
- [16] Xiao Yu. Study on bending performance of concrete composite slabs using semi-prefabricated slabs without extended bars[D]. Xuzhou: China University of Mining and Technology, 2021. [肖宇. 预制底板不出筋的混凝土叠合板的受弯性能研究[D]. 徐州:中国矿业大学,2021.]
- [17] Lan feng. Experimental research on joint performance of concrete composite slabs without extended bars on the side[D]. Guangzhou: South China University of Technology, 2022. [蓝丰. 板侧不出筋混凝土叠合板拼缝连接性能试验研究[D]. 广州:华南理工大学,2022.]
- [18] Xie Zhongshu. Mechanical properties test and elaborate numerical modeling of lattice girder composite slab with monolithic joints[D]. Hangzhou: Zhejiang Sci-Tech University, 2022. [解忠舒. 密拼钢筋桁架叠合板力学性能试验及精细化有限元分析[D]. 杭州:浙江理工大学,2022.]
- [19] Lv Ying. Study on anchoring and noncontact lap splice performance of rebars in concrete composite slab.[D]. Beijing: Tsinghua University, 2021. [吕颖. 叠合板中钢筋的锚固与间接搭接性能研究[D]. 北京:清华大学,2021.]
- [20] Zhang Xuefeng, Zheng Shuguang, Shan Yuchuan, et al. Experimental study on full-scale steel bar truss superimposed two-way slabs without extending reinforcement on all sides and connected without gap[J]. Building Structure, 2019,49(15):83–87. [章雪峰,郑曙光,单玉川,等. 四边不出筋密拼连接叠合双向板足尺试验研究[J]. 建筑结构, 2019,49(15):83–87.]
- [21] Xiao Yu, Li Xian. Experimental study on bending performance of concrete composite slabs using new connection joints without extended bars[J]. Building Structure, 2023,53(5):83–89. [肖宇,李贤. 新型不出筋拼缝混凝土叠合板受弯性能试验研究[J]. 建筑结构,2023,53(5):83–89.]
- [22] Jiang Haihua. Study on the performance of a flat plate composite plate with no reinforcement at the end of the plate [D]. Chongqing: Chongqing University, 2022. [江海华. 一种板端不出筋的平板叠合板性能研究[D]. 重庆:重庆大学, 2022.]
- [23] 中华人民共和国住房和城乡建设部. 混凝土结构实验方法标准:GB/T 50152—2012[S]. 北京:中国建筑工业出版社,2012.
- [24] Wang Shi, Wang Lihua, Wang Bin, et al. Optimization and mechanical performance analysis of laminated plate truss [J]. Journal of Shandong Jianzhu University, 2023,38(2):32–39. [王示,王丽华,王斌,等. 叠合板桁架的优化及力学性能分析[J]. 山东建筑大学学报,2023,38(2):32–39.]

Experimental Study on Bearing Capacity of Full-scale Composite Slabs with L-shaped Rabbet

LIU Wei^{1,2}, GUO Xiaonong¹, WEN Yi³, WANG Bing², ZHOU Sen², XU Jun³, DAI Kaoshan^{3*}

(1.College of Civil Engineering, Tongji University, Shanghai 200092, China; 2.Shanghai Baoye Group Co., Ltd., Shanghai 200941, China;

3.Department of Civil Engineering, Sichuan University, Chengdu 610065, China)

Abstract:

Objective Traditional composite slabs require protruding reinforcement bars in the prefabricated base plate during production to ensure the integrity of the interface between joints and beam-panel connections. However, these protruding bars hinder the handling and stacking of components, adversely affecting on-site construction and component quality. Therefore, this study proposes a construction method for composite slabs with an L-shaped rabbet that eliminates the need for protruding reinforcement bars.

Methods This study conducted static loading tests on six full-scale floor slab specimens with end beams to investigate the effect of the L-shaped rabbet end design method on the integrity of beam-panel connections and the bearing capacity of composite slabs. The specimens consisted of three composite slabs with L-shaped rabbets (design method one), two traditional composite slabs, and one cast-in-place solid slab with the same dimensions. The L-shaped rabbet composite slabs served as the experimental group, while the remaining slabs were designed traditionally and served as control groups 1 and 2, respectively. The study compared the load-bearing capacity and crack resistance of the new slabs. The loading was applied by stacking weights, with each weight block weighing 1 ton (900 kg). Each floor slab accommodated up to nine weight blocks in a single layer. The loading sequence followed a centrally symmetrical pattern to ensure even stress distribution during testing. The measurement parameters during the test included: 1) the number of weight blocks applied; 2) vertical displacement at the mid-span and on the upper part of beams, and horizontal displacement at the lower part of beams; 3) strain of reinforcing bars under stress; and 4) crack width at the mid-span and at the interface between the slab and beams. Strain gauges were attached to the reinforcing bars on the upper and lower surfaces of the composite slabs. Displacement meters were installed at the slab ends, mid-span, along the beam edges, and at the top. Crack depth and width were observed using a crack depth-width gauge under various loading conditions. Instruments such as strain acquisition devices, high-precision displacement meters, and crack observation tools were utilized to collect data from critical areas of the specimens. These included strain on L-shaped reinforcement at the ends, strain on protruding reinforcement at the ends of traditional composite slabs, deflection at the mid-span of composite slabs, and

crack widths and spacings at the mid-span. These data provided a detailed basis for analyzing the overall performance of the floor slabs and the local performance of steel and concrete components.

Results and Discussions Upon analyzing the experimental results, the study evaluated the number, spacing, and width of mid-span cracks, as well as the width of end cracks, as observation indicators. The crack development process in each group of slabs was similar. Cracks initially appeared at the locations of maximum bending moments at the slab ends and mid-span. As the load increased, both the number and width of mid-span cracks increased continuously, with smaller crack spacing and transversely extending cracks, exhibiting typical flexural failure characteristics. Regarding the number of cracks, the new slabs had an average of 13.3 mid-span cracks, close to the 14 cracks observed in traditional slabs. In terms of crack spacing, the average spacing for the new slabs was 10.96 cm compared to 9.275 cm for the traditional slabs, indicating a small difference. This finding indicated that, compared to traditional slabs, the new end construction did not reduce the bearing capacity at the mid-span. Regarding crack width at the slab ends, under a uniformly distributed load of 27.9 kN/m^2 , the end crack width at each sampling point indicated that the new slabs exhibited similar crack widths to traditional slabs and performed significantly better than the cast-in-place slabs. This similarity was evident from the crack width data and the consistent changes in the curve slopes between the two slab types, confirming that the L-shaped rabbet end design provided comparable overall integrity at the beam-panel connections to that of the traditional protruding reinforcement method in composite slabs. Regarding deflection, the mid-span deflection was considered the representative value. The development of deflection in the new slabs was similar to that of the traditional slabs. The rate of deflection increase in the new slabs was slightly lower than that in traditional slabs, and the deflection at the limit state of bearing capacity was also lower, while the cast-in-place slab demonstrated the lowest stiffness. Based on a comprehensive analysis of deflection and cracking behavior, the end construction with L-shaped reinforcement did not significantly affect the bending stiffness at the mid-span of composite slabs. Regarding strain, similar to traditional reinforcement, the L-shaped reinforcement experienced minimal compressive stress during normal use, particularly before concrete cracking, and contributed little to the bending capacity at the member ends. As the height of the compressed zone decreased, the L-shaped reinforcement at the ends began to bear tensile stress. In the later stages of loading, both the L-shaped reinforcement in the new slabs and the protruding reinforcement in traditional slabs yielded, fully utilizing the load-bearing capacity of the reinforcement. The design of the L-shaped rabbet compensated for the potential reduction in bond strength caused by the shorter length of the L-shaped reinforcement.

Conclusions The width and distribution of end cracks in the new slabs are highly similar to those in traditional slabs and significantly better than those in cast-in-place slabs using the L-shaped rabbet during the loading process. This finding indicates that the L-shaped end design method provides sufficient reliability in beam-panel connections. The L-shaped bend restricts relative slippage between the reinforcement and the concrete, ensuring a stable connection between the slab end and the main beam. It compensates for the potentially low bond strength caused by the shorter length of the L-shaped reinforcement, enhancing structural safety. The load-bearing capacity of the new slabs did not significantly decrease and was equivalent or nearly equivalent to that of traditional protruding reinforcement composite slabs, satisfying the requirements for normal service limit state and ultimate limit state conditions. This preliminary validation confirms the feasibility of the L-shaped rabbet design for composite slabs without protruding reinforcement at the ends.

Key words: composite slab without extended bars; full-scale test; L-shaped groove; mechanical performance; beam-slab interface

(编辑 张 琼)

引用格式: Liu Wei, Guo Xiaonong, Wen Yi, et al. Experimental study on bearing capacity of full-scale composite slabs with L-shaped rabbet[J]. *Advanced Engineering Sciences*, 2025, 57(6): 213–221. [刘威, 郭小农, 文艺, 等. “L”形槽不出筋叠合板承载性能足尺试验研究[J]. *工程科学与技术*, 2025, 57(6): 213–221.]